BMP4-mediated brown fat-like changes in white adipose tissue alter glucose and energy homeostasis

Shu-Wen Qian[a,b], Yan Tang[a], Xi Li[a,b], Yuan Liu[b], You-You Zhang[b], Hai-Yan Huang[a,b], Rui-Dan Xue[c], Hao-Yong Yu[d,e], Liang Guo[a], Hui-Di Gao[a], Yan Liu[b], Xia Sun[b], Yi-Ming Li[c], Wei-Ping Jia[d,e], and Qi-Qun Tang[a,b,1]

[a]Key Laboratory of Molecular Medicine, the Ministry of Education, Department of Biochemistry and Molecular Biology, Fudan University Shanghai Medical College, Shanghai 200032, People's Republic of China; [b]Institute of Stem Cell Research and Regenerative Medicine, Institutes of Biomedical Sciences, Fudan University, Shanghai 200032, People's Republic of China; [c]Division of Endocrinology and Metabolism, Department of Internal Medicine, Huashan Hospital, Fudan University Shanghai Medical College, Shanghai 200040, People's Republic of China; [d]Department of Endocrinology and Metabolism, Shanghai Clinical Center for Diabetes, Shanghai Jiaotong University Affiliated Sixth People's Hospital, Shanghai 200233, People's Republic of China; and [e]Shanghai Diabetes Institute, Shanghai Key Laboratory of Diabetes Mellitus, Shanghai 200233, People's Republic of China

Edited by M. Daniel Lane, The Johns Hopkins University School of Medicine, Baltimore, MD, and approved January 17, 2013 (received for review September 5, 2012)

Expression of bone morphogenetic protein 4 (BMP4) in adipocytes of white adipose tissue (WAT) produces "white adipocytes" with characteristics of brown fat and leads to a reduction of adiposity and its metabolic complications. Although BMP4 is known to induce commitment of pluripotent stem cells to the adipocyte lineage by producing cells that possess the characteristics of preadipocytes, its effects on the mature white adipocyte phenotype and function were unknown. Forced expression of a BMP4 transgene in white adipocytes of mice gives rise to reduced WAT mass and white adipocyte size along with an increased number of a white adipocyte cell types with brown adipocyte characteristics comparable to those of beige or brite adipocytes. These changes correlate closely with increased energy expenditure, improved insulin sensitivity, and protection against diet-induced obesity and diabetes. Conversely, BMP4-deficient mice exhibit enlarged white adipocyte morphology and impaired insulin sensitivity. We identify peroxisome proliferator-activated receptor gamma coactivator 1-α (PGC1α) as the target of BMP signaling required for these brown fat-like changes in WAT. This effect of BMP4 on WAT appears to extend to human adipose tissue, because the level of expression of BMP4 in WAT correlates inversely with body mass index. These findings provide a genetic and metabolic basis for BMP4's role in altering insulin sensitivity by affecting WAT development.

adipocyte terminal differentiation | brown adipose tissue | mitochondria | metabolism

Both white adipose tissue (WAT) and brown adipose tissue (BAT) function in the energy homeostasis of humans and other mammals. WAT stores energy in form of triglycerides during periods of excessive caloric intake for later use when energy demand exceeds intake (1). In contrast, brown adipose tissue (BAT) uses "stored triglycerides" to generate energy in the form of heat, most notably when environmental temperature falls (2).

The excessive accumulation of body fat in WAT is the result of both hypertrophy and hyperplasia of white adipocytes (3). Such changes give rise to insulin resistance, type-2 diabetes, and an inflammatory response, thus implicating white adipocytes in the etiology of these conditions (4, 5). In contrast, promotion of BAT activities helps prevent genetic obesity, insulin resistance, and diabetes (6).

Unlike the expansive mass of brown adipocytes in the interscapular region, brown adipose tissue mass in the normal adult human is proportionally smaller and previously was believed to be functionally less important. Recently, however, by using [18F]-2-fluoro-D-2-deoxy-D-glucose PET, metabolically active regions were detected in the cervical, supraclavicular, axillary, and paravertebral regions of adult human subjects (7–9). The metabolically active areas were found to consist of an admixture of brown-like adipocytes in WAT (10) which increase dramatically following cold exposure or treatment with antidiabetic drugs, thiazolidinediones, or adrenergic activators (11–13). These cells recently have been designated as "beige" (14) or "brite" (15, 16) cells derived from lineages different from classical brown fat cell precursors. Moreover, the number of BAT-like cells is inversely correlated with body mass index (BMI) in humans (17). Identification of the factors that induce brown-like fat cells in WAT could provide an approach for the prevention and/or treatment of obesity and its metabolic complications.

Recently, mouse models have become available with specific genetic manipulations that produce a lean phenotype with lower WAT mass and enhanced insulin sensitivity (18–20). The WAT of these mice possesses some characteristics of BAT, notably increased mitochondrial biogenesis and metabolic rate. Perturbed mitochondrial oxidation in muscle and liver is thought to cause insulin resistance and type 2 diabetes in several human studies (21–23). Adipose tissue of obese (ob/ob) mice exhibits decreased mitochondrial gene expression and mitochondrial mass that can be reversed by treatment with the peroxisome proliferator-activated receptor γ (PPARγ) agonist rosiglitazone (12). These findings indicate that mitochondrial remodeling and increased energy expenditure in white fat also can affect whole-body energy homeostasis and insulin sensitivity. As previously reported, PPARγ coactivator α (PGC1α) is a key mitochondrial-related transcription factor that mediates coactivation of key nuclear hormone receptor-dependent gene transcription as well as mitochondria biogenesis (24–28), which is known to be involved in glucose and fatty acid metabolism.

Down-regulation of PGC1α is associated with obesity and increased risk of diabetes mellitus in the human population (29). Several members of the bone morphogenic protein (BMP) family have been reported to act differently on adipocyte lineages. BMP7 induces the brown preadipocytes to differentiate but has no effect on white preadipocytes (30). More recently, BMP8B was found to function in mature brown adipocytes to increase lipase activity, which facilitates a thermogenic response (31).

Our previous studies show that BMP4 induces multipotent mouse C3H10T1/2 stem cells to become a cell type with characteristics identical to those of 3T3-L1 white preadipocytes in culture (32). In the present study, we show that BMP4 is expressed at an elevated level in WAT of lean human subjects.

Author contributions: S.-W.Q. and Q.-Q.T. designed research; S.-W.Q., Y.T., Yuan Liu, R.-D.X., H.-Y.Y., L.G., H.-D.G., Yan Liu, and X.S. performed research; S.-W.Q., X.L., Y.-Y.Z., H.-Y.H., Y.-M.L., W.-P.J., and Q.-Q.T. analyzed data; and S.-W.Q. and Q.-Q.T. wrote the paper.

The authors declare no conflict of interest.

This article is a PNAS Direct Submission.

[1]To whom correspondence should be addressed. E-mail: qqtang@shmu.edu.cn.

See Author Summary on page 3223 (volume 110, number 9).

This article contains supporting information online at www.pnas.org/lookup/suppl/doi:10.1073/pnas.1215236110/-/DCSupplemental.

Our findings with adipose-targeted BMP4 overexpression and knockout in mice suggest that BMP4 can regulate WAT remodeling and induction of brown adipocyte-like cell structure and function. These alterations lead to increases in whole-body metabolic rate and insulin sensitivity. We found that PGC1α acts as a key regulator that is transactivated by activating transcription factor 2 (ATF2) mainly through the BMP4–p38/MAPK signaling pathway. Our findings reveal a role for BMP4 in regulating adipogenesis and metabolism.

Results

Elevated Expression of BMP4 in WAT Correlates with a Lean Phenotype. Our previous studies showed that BMP4 induces commitment of stem cells to the adipocyte lineage in mice (32). As shown below, expression of BMP4 also alters the WAT phenotype in mice. The question arises whether BMP4 functions similarly in humans. As illustrated in Fig. 1 *A* and *B*, BMP4 is expressed both in human subcutaneous and visceral WAT. Moreover, the level of expression of BMP4 in human WAT is inversely correlated to adiposity, i.e., BMI. These results suggested that BMP4 might regulate adipocyte development and its metabolic consequences.

Induced Expression of BMP4 in WAT Produces a BAT-Like Phenotype. To assess the effect of expressing BMP4 in adipocytes, transgenic (TG) mice were generated using the adipose tissue-specific fatty acid-binding protein 4 (Fabp4) promoter to drive the expression of BMP4 (Fig. S1*A*). As shown in Fig. 1*C* and Fig. S1*B*, BMP4

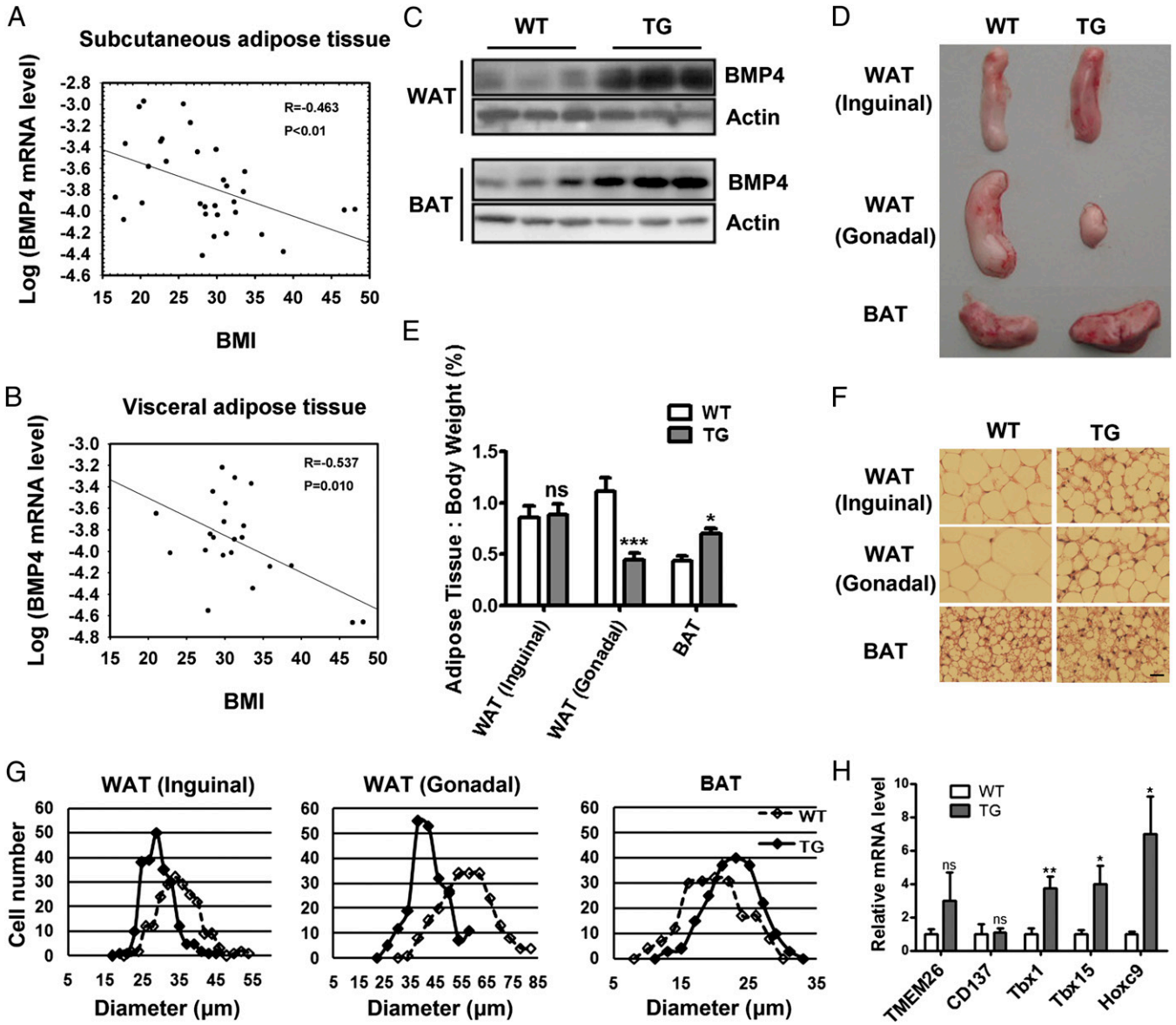

Fig. 1. High expression of BMP4 remodels WAT and produces a lean phenotype. (*A* and *B*) Linear regression analysis between BMI and BMP4 mRNA levels in subcutaneous ($n = 32$) (*A*) and visceral ($n = 22$) (*B*) adipose tissue. (*C*) Western blot analysis of BMP4 expression levels in WAT and BAT from WT and Fabp4-BMP4 TG mice. (*D*) Comparison of inguinal WAT, gonadal WAT, and BAT from WT (*Left*) and TG (*Right*) mice. (*E*) Fat index (percentage of fat pad weight relative to the whole body weight) of inguinal WAT, gonadal WAT, and BAT in WT and TG mice ($n = 4$). (*F*) H&E staining of inguinal WAT, gonadal WAT, and BAT from WT and TG mice. (Scale bar: 20 μm.) (*G*) Quantification of adipocyte diameter of inguinal WAT, gonadal WAT, and BAT from WT and TG mice. (Data were collected from H&E-stained sections from three individual mice, five fields per mouse, 10–15 cells per field in each group, using Image J software). (*H*) qRT-PCR data showing the fold induction of indicated genes with expression normalized to the housekeeping gene 18S in inguinal WAT of WT and TG mice ($n = 8$). Data from 2-mo-old mice on a normal chow diet are expressed as means ± SEM. $^*P < 0.05$, $^{**}P < 0.01$, $^{***}P < 0.001$.

expression was increased in both WAT and BAT of the TG mice. Expression of BMP4 in the stromal vascular fraction (SVF) was not affected by the transgene (Fig. S1*C*). Although the Fabp4 promoter has been shown to be active in the brain (33), the BMP4 mRNA level was not elevated in brain by the transgene (Fig. S1*D*).There was no significant difference in BMP4 expression in muscle and liver tissue of TG relative to control mice (Fig. S1*E*). Thus, expression of BMP4 in the TG mice was limited to adipose tissue.

The amount of gonadal (visceral) WAT was reduced markedly by the BMP4 transgene in both male and female mice (Fig. 1 *D* and *E*; and Fig. S1*F*). However, the amount of inguinal (subcutaneous) WAT obviously remained unchanged (Fig. 1 *D* and 1*E* and Fig. S1*F*). Moreover, the inguinal WAT tissue acquired a reddish appearance characteristic of BAT (Fig. 1 *D* and *F*). The amount of interscapular BAT increased slightly (Fig. 1 *D* and *E* and Fig. S1*F*). The size of both inguinal and gonadal adipocytes was reduced in the BMP4 TG mice, and the cells lost their unilocular morphology and acquired a multilocular appearance (Fig. 1 *F* and *G*). These results indicated that the expression of a high level of BMP4 in WAT led to a BAT-like appearance. Furthermore, the expression of beige adipocyte markers or factors reported to be highly expressed in beige/brite adipocytes (14–16), i.e., CD137, transmembrane protein 26 (TMEM26), transcription factor T-box 1 (Tbx1), transcription factor T-box 15 (Tbx15), and homeo box C9 (Hoxc9),

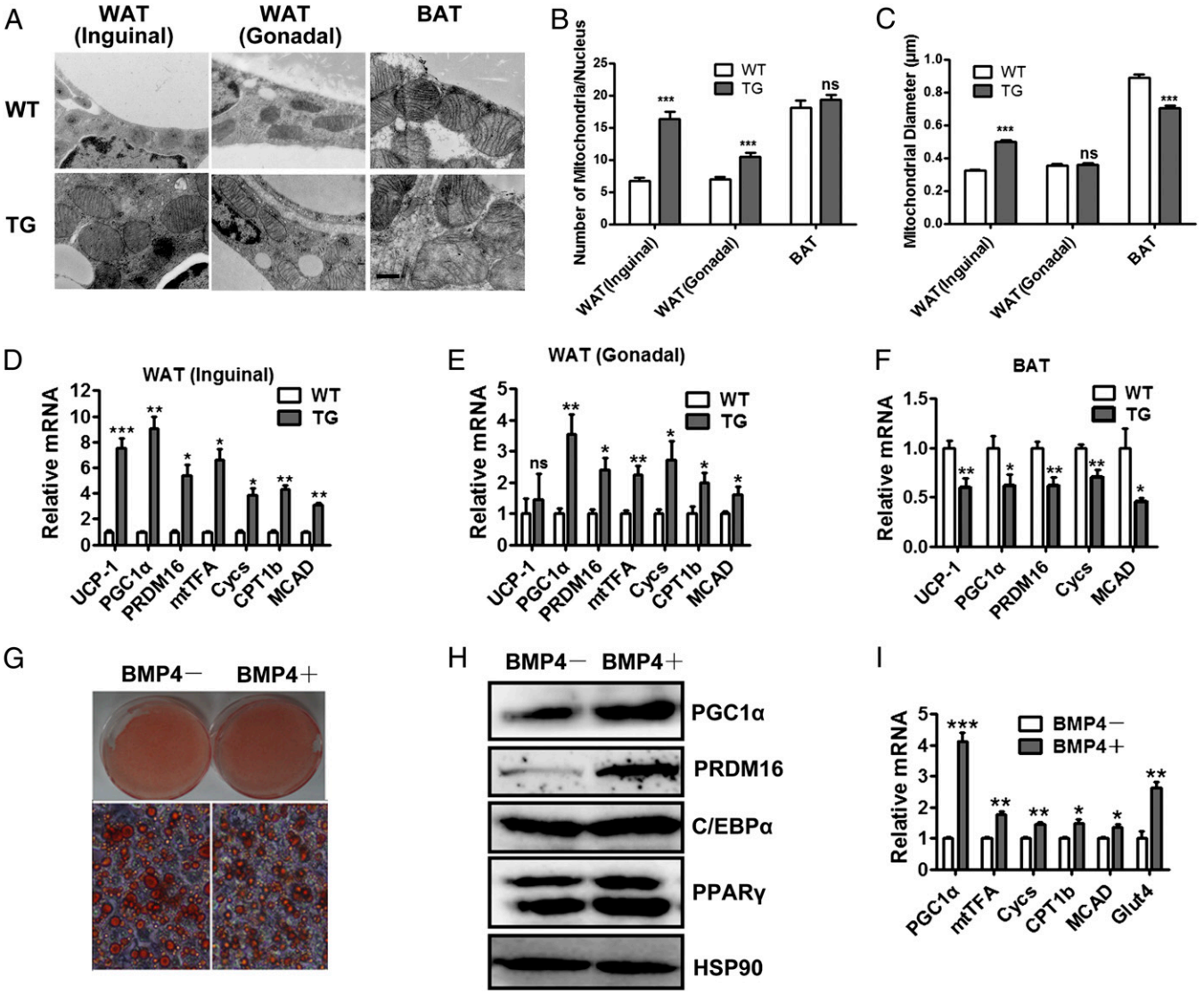

Fig. 2. Increased mitochondrial biogenesis of WAT in Fabp4-BMP4 TG mice. (*A*) Transmission electron microscopy showing mitochondrial morphology of WAT and BAT from WT and Fabp4-BMP4 TG mice. (Scale bar: 500 nm.) (*B*) Mitochondrial number per nucleus was determined from electron micrographs of 20 cells from each type of adipose tissue. (*C*) Mitochondria (120–150) were randomly selected, and mitochondrial diameter was determined with a ruler. (*D*) qRT-PCR data showing the fold induction of the expression of indicated genes normalized to the housekeeping gene 18S in inguinal WAT of WT and TG mice (n = 4–6). (*E*) qRT-PCR data showing the fold induction of the expression of the indicated genes normalized to the housekeeping gene 18S in gonadal WAT of WT and TG mice (n = 4–7). (*F*) qRT-PCR data showing the fold induction of the expression of the indicated genes normalized to the housekeeping gene 18S in BAT of WT and TG mice (n = 4–7). (*G*) Arrest of postconfluent growth. 3T3-L1 preadipocytes were induced to differentiate by treatment with monocyte differentiation-inducing factors (MDI) with or without 20 ng/mL BMP4. Adipocytes differentiated from 3T3-L1 adipocytes at day 8 after MDI induction are stained with Oil Red O. (*H*) Western blot analysis of lysates (30 μg) differentiated from 3T3-L1 adipocytes at day 6 after MDI induction with or without 20 ng/mL BMP4. (*I*) qRT-PCR of differentiated 3T3-L1 adipocytes for expression of indicated genes at day 6 after MDI induction with or without 20 ng/mL BMP4. Data from 2-mo-old mice on a normal chow diet are expressed as means ± SEM. $^{*}P < 0.05$, $^{**}P < 0.01$, $^{***}P < 0.001$.

was examined. The mRNA levels of TMEM26 and CD137 did not increase significantly, but Tbx1, Tbx15, and Hoxc9 levels increased in the inguinal WAT of BMP4 TG mice (Fig. 1*H*).

Although the percentage of mature adipocytes relative to total cell number in the fat tissue mass in both WAT and BAT did not differ between the two types of mice (Fig. S1*G*), the number (based on DNA content) of inguinal white and brown adipocytes increased, whereas the number of gonadal white adipocytes remained unchanged (Fig. S1*H*). Thus, both inguinal WAT and BAT underwent BMP4-induced hyperplasia.

Induced Expression of BMP4 Leads to Increased Mitochondrial Biogenesis and Key BAT Gene Expression in WAT. Because subcutaneous inguinal WAT of the BMP4 TG mice acquired the appearance of BAT, we investigated the possibility that mitochondrial biogenesis in WAT occurred. Immunohistochemical analysis showed more mitochondria staining immunopositive in both inguinal and gonadal WAT of TG mice (Fig. S2*D*). Transmission electron microscopy of inguinal WAT revealed a marked increase in the number and size of mitochondria (Fig. 2 *A*–*C*). Although the diameters of mitochondrial organelles in gonadal WAT did not change significantly, the number did increase (Fig. 2 *A*–*C*).

PGC1α and PR domain containing 16 (PRDM16) are regarded as key inducers of brown adipocyte development (34–37). Real-time PCR analysis revealed that levels of PGC1α and uncoupling protein 1 (UCP1) (a target gene of PGC1α) were increased approximately ninefold and approximately 7.5-fold, respectively, whereas PRDM16 was increased approximately sixfold in inguinal WAT of BMP4 TG mice (Fig. 2*D*). Consistent with these changes, the levels of the mRNAs encoding mitochondrial cytochrome C (Cycs), mitochondrial transcription factor A (mtTFA), carnitine palmitoyl-CoA:transferase 1B (CPT1b), and medium-chain acyl-CoA dehydrogenase (MCAD) were elevated in BMP4 TG mice (Fig. 2*D*). Except for UCP-1, the expression of these brown adipocyte developmental- and mitochondrial-related genes also was increased in gonadal WAT (Fig. 2*E*). In BAT, however, the expression of these genes decreased in BMP4 TG mice (Fig. 2*F*), as did mitochondrial size. However, the number of mitochondria did not change (based on electron microscopic measurements; Fig. 2 *B* and *C*), and fewer mitochondria exhibited immunopositive staining by immunohistochemical analysis (Fig. S2*D*).

Although BMP4 treatment during terminal differentiation in the 3T3-L1 preadipocyte culture model did not affect differentiation efficiency significantly, as indicated by the expression of adipocyte marker proteins CCAAT/enhancer-binding protein α (C/EBPα) and PPARγ or by Oil Red O staining of adipocytes (Fig. 2 *G* and *H*). Moreover, the accumulated lipid droplets were smaller in the BMP4-treated cells than in controls as determined by the appearance of micrographic images after Oil Red staining (Fig. 2*G*). In addition, the BMP4-treated 3T3-L1 adipocytes also acquired the brown adipocyte gene expression phenotype, including the expression of PGC1α and PRDM16 (Fig. 2 *H* and *I*) as well as downstream genes, i.e., mtTFA, Cycs, CPT1b, MCAD, and glutamate transporter type 4 (Glut4) (Fig. 2*I*). The expression of UCP-1 could not be detected readily by Western blotting or with a high cycle threshold value (>30) by real-time PCR. Although the relative level of expression of PGC1a was high, the level ofUCP-1 expression was unexpectedly low.

Elevated Expression of BMP4 in Adipose Tissue Increases Whole-Body Oxygen Consumption, Insulin Sensitivity, and Protection from Metabolic Disorders Induced by a High-Fat Diet. Basal oxygen consumption rates of BMP4 TG mice were increased substantially relative to those of control mice (Fig. 3 *A* and *B*). The mean respiratory exchange ratio (RER) of TG mice was 0.72 and that of WT mice was 0.83, indicating that the TG mice were oxidizing primarily fat, whereas the WT mice were oxidizing a mixture of carbohydrate and fat (Fig. 3*C*). Consistent with this shift to fat as primary fuel, the circulating levels of both triglycerides and free fatty acid decreased substantially in the BMP4 TG mice compared with control mice (Fig. 3*D*). Serum cholesterol levels were unchanged by expression of the transgene (Fig. 3*D*).

The increase in fat metabolism by WAT in BMP4 TG mice and the associated reduction in the level of circulatory fat metabolites suggested that the BMP4 TG mice might be more insulin responsive (38). To test this possibility, metabolic studies were performed in which BMP4 TG and WT mice were fed either chow or a high-fat diet (HFD) from age 6–24 wk. Of interest, the BMP4 TG mice consumed slightly more of both diets than control mice (Fig. 3*E*). Body weights of the mice fed the chow diet began to diverge at approximately age 8 wk, with the TG mice gaining somewhat more weight than control mice between age 10 and 24 wk (Fig. 3*F*). Nonetheless, the size of the inguinal WAT fat pad increased (Fig. S2*E*), and the fat cells were small in size and were multilocular at age 24 wk (Fig. S2*F*). The difference in body weight was less pronounced in TG and control mice on the HFD (Fig. 3*F*). Although the fat pads of TG mice increased in size upon exposure to the HFD, the increase was less than in control mice, and fewer lipids accumulated in the liver (Fig. S2 *E* and *F*).

When mice were maintained on the chow diet, the BMP4 TG mice exhibited lower fasting serum glucose and insulin levels than control mice (Fig. 3 *G* and *H*). The fasting glucose and insulin levels were significantly increased in mice on the HFD (Fig. 3 *G* and *H*), but the levels of serum glucose and insulin were significantly reduced in BMP4 TG mice relative to controls (Fig. 3 *G* and *H*), suggesting increased insulin sensitivity. When challenged with an i.p. glucose load, the BMP4 TG mice on both chow and HFD displayed significantly improved glucose tolerance. Intraperitoneal insulin tolerance tests also showed improved insulin sensitivity in Fabp4-BMP4 mice (Fig. 3 *I* and *J*). Finally, i.p. injection of insulin resulted in a more pronounced activation of the insulin-signaling pathway in WAT of the BMP4 TG mice, as indicated by the relative increase in the level of phosphorylated Akt (phospho-Akt) (Fig. 3*K*).

PGC1α Mediates BMP4-Induced Conversion of White Adipocytes into Brown Fat-Like Adipocytes. PGC1α is an important transcriptional coactivator for the expression of the UCP-1 gene (39), for the biogenesis of mitochondria, and for energy expenditure in BAT and other tissues (24, 26). To determine whether the increased energy expenditure and improved insulin sensitivity of the BMP4 TG mice is dependent on PGC1α, recombinant adenovirus expressing PGC1α shRNA was injected s.c. adjacent to one inguinal fat pad site. As a control, recombinant adenovirus expressing LacZ shRNA was injected in the contralateral site. Injection of adeno-PGC1α-shRNA into the white fat pads of BMP4 TG mice caused a significant decrease in PGC1α mRNA level compared with the contralateral control. Likewise, CPT1b, MCAD, and phosphoenolpyruvate carboxykinase 1 (Pck-1) were down-regulated (Fig. 4*C*). The knockdown of PGC1α expression in the fat pads produced a lighter color than in the reddish contralateral control fat pads (Fig. 4*A*) as well as enlargement of the fat cells and fat droplets (Fig. 4*B*). Thus, the phenotype induced in the BMP4 TG mice was reversed by knocking down the expression of PGC1α. Finally, activation of the insulin-signaling pathway also was inhibited by PGC1α knockdown (Fig. 4*D*). Moreover, regression analysis revealed a positive association between BMP4 and PGC1α mRNA expression in both subcutaneous ($n = 32$) and visceral ($n = 22$) adipose tissue of human subjects (Fig. 4 *E* and *F*).

P38/MAPK/ATF2 Pathway Regulates the BMP4-Induced BAT-Like Change in WAT. Two major signaling pathways, the Smad (mothers against decapentaplegic homolog) and p38/MAPK pathways, are known for BMPs (40). Overexpression of BMP4 in WAT in-

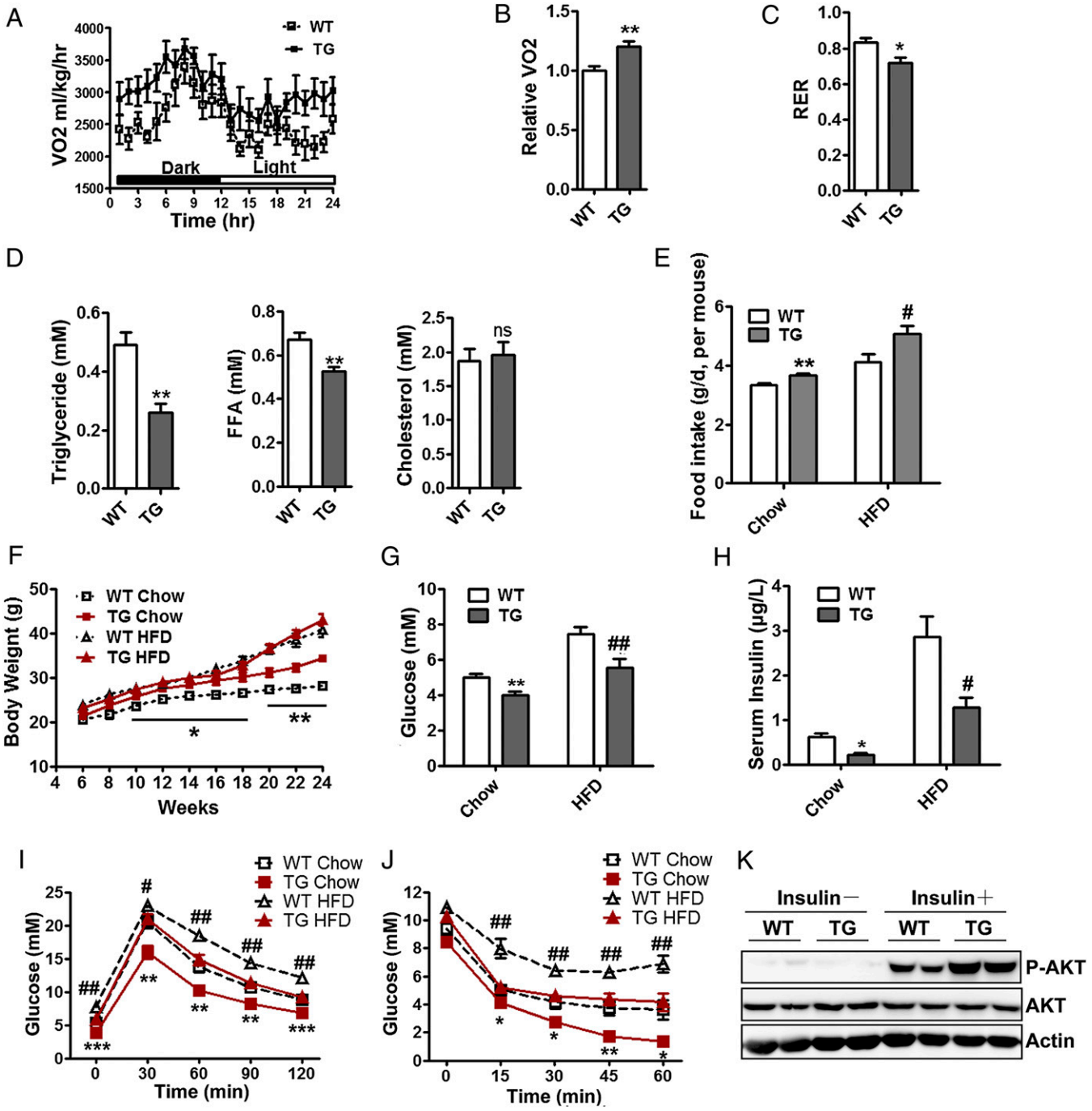

Fig. 3. Energy expenditure and glucose metabolism in BMP4 TG mice. (*A* and *B*) Whole-body oxygen consumption rate (VO2) of WT and TG mice during a 12-h dark/12-h light cycle measured in a metabolic cage (*A*) and the average values for the 24-h period (*B*). $n = 8$. (*C*) The average values of RER in WT and TG mice calculated from data from the metabolic cage ($n = 8$). (*D*) Fasting serum triglycerides ($n = 6$), free fatty acid (FFA) ($n = 9$), and cholesterol ($n = 6$) levels in WT and TG mice. (*E*) Daily food intake of WT and Fabp4-BMP4 TG mice maintained on chow or an HFD. Mice were weighed each week for 4 wk. $n = 12$ mice per group. (*F*) Body weight gain of WT and TG mice maintained on chow or an HFD. $n = 4$ mice per group. (*G* and *H*) Fasting serum glucose ($n = 6$) (*G*) and insulin concentrations ($n = 6$) (*H*) in WT and TG mice maintained on chow or an HFD. (*I* and *J*) Glucose concentrations during an i.p. glucose tolerance test ($n = 8$) (*I*) or an insulin tolerance test ($n = 7$) (*J*) in WT and TG mice maintained on chow or an HFD. (*K*) Western blot analysis of insulin-stimulated phosphorylation of AKT in inguinal WAT extracts from WT and TG 6-mo-old mice maintained on chow. Data are expressed as means ± SEM. For WT vs. TG mice fed chow: $^{*}P < 0.05$, $^{**}P < 0.01$, $^{***}P < 0.001$; for WT vs. TG mice fed a high-fat diet: $^{\#}P < 0.05$, $^{\#\#}P < 0.01$, $^{\#\#\#}P < 0.001$. (Twenty-four-week-old mice were maintained on chow or were fed an HFD beginning at age 6 wk.)

creased the phosphorylation state of both p38/MAPK and phosphorylated Samd1/5/8 (p-Samd1/5/8) (Fig. 5*A*). Because ATF2 lies downstream of p38/MAPK, its expression level also was assessed by Western blotting. Both phosphorylated ATF2 (P-ATF2) and ATF2 protein levels were up-regulated in WAT of BMP4 TG mice (Fig. 5*A*), suggesting that BMP4 plays a role not only in the activation of ATF2 but also the expression of the protein itself (Fig. 5*A*). Moreover, knockdown of ATF2 expression in inguinal WAT of BMP4 TG mice reversed the effect of BMP4 on WAT, causing fat cell enlargement and decreased expression of PGC1α

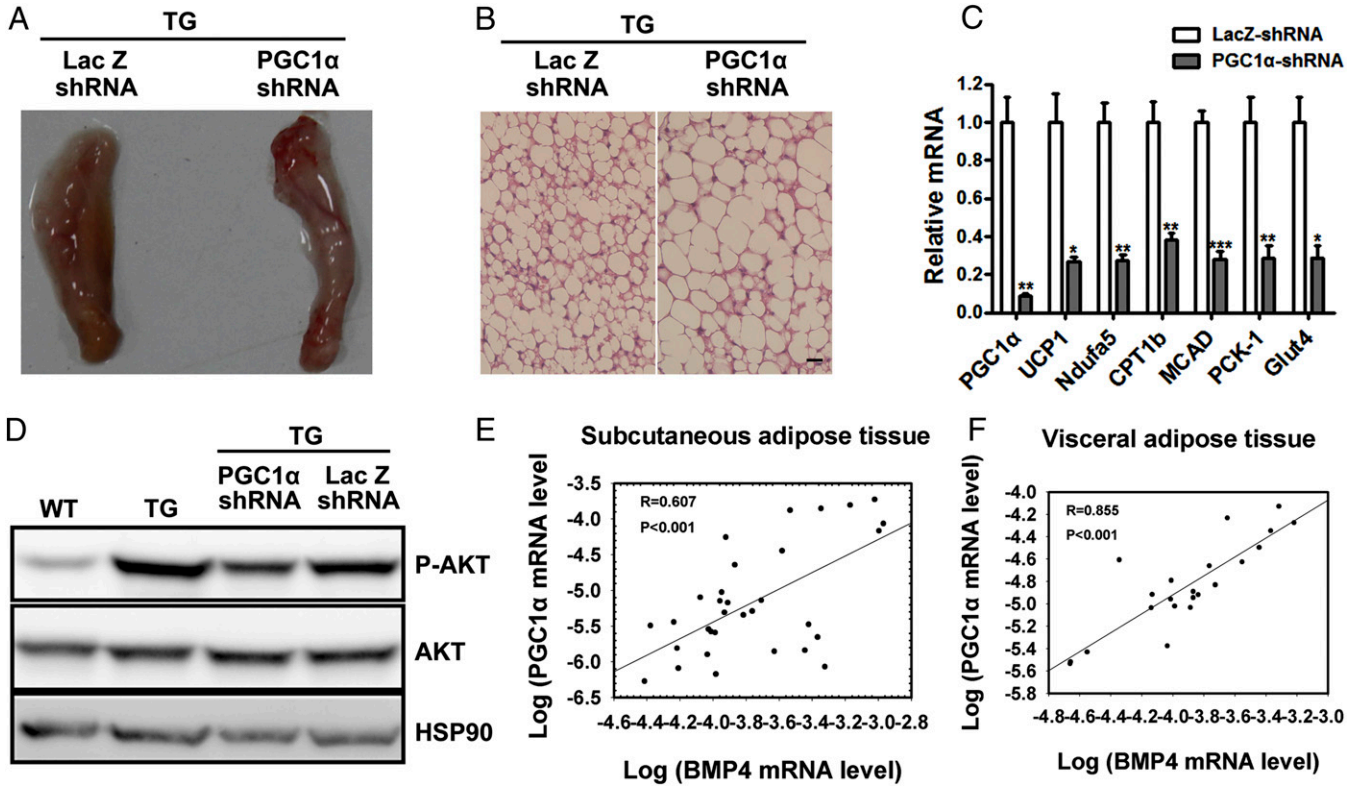

Fig. 4. Active metabolic WAT in Fabp4-BMP4 TG mice is dependent on PGC1α. Adenovirus expressing PGC1α shRNA was injected weekly s.c. adjacent to one side of the inguinal fat pad, and LacZ shRNA was injected at the contralateral site as a control for 4 wk beginning at age 4 wk. (*A*) Comparison of inguinal WAT fat pads in the TG mouse after treatment with PGC1α or Lac Z shRNA. (*B*) H&E staining of the inguinal WAT fat pad in the TG mouse after treatment with PGC1α or Lac Z shRNA. (Scale bar: 20 μm.) (*C*) qRT-PCR showing the fold induction of the expression of the indicated genes normalized to the housekeeping gene 18S in the inguinal WAT fat pad in the TG mouse after treatment with PGC1α or Lac Z shRNA (n = 4). (*D*) Western blot analyzing insulin-stimulated phosphorylation of AKT from the inguinal WAT fat pad in the TG mouse after treatment with PGC1α or Lac Z shRNA. (*E* and *F*) Linear regression analysis between BMP4 and PGC1α mRNA levels in subcutaneous (n = 32) (*E*) and visceral (n = 22) (*F*) adipose tissue.

and UCP-1 in fat pads injected with adeno-AFT2 shRNA compared with contralateral control fat pads (Fig. 5 *B* and *C*). The activating signaling by BMP4 on WAT was recapitulated in terminally differentiating 3T3-L1 cells in culture (Fig. 5*D*). Together these findings showed that activation of the p38/MAPK/ATF2 pathway and the activation of PGC1α expression by BMP4 play important roles in the induction of WAT into BAT-like tissue. Although a different phenotype was induced by the BMP4 transgene in WAT, BMP4 overexpression in BAT also activated the p38/MAPK/ATF2 pathway (Fig. S2*G*).

Disruption of BMP4 Expression in Adipose Tissue Increases Adipose Tissue Mass and Reduces Insulin Responsiveness. To determine whether the effect of BMP4 on adipocyte phenotype is reversible, mice with an adipose tissue BMP4 knockout were used (Fig. S3*A*). Knockout mice were prepared by crossing Fabp4-driven Cre recombinase mice with $BMP4^{loxP/loxP}$ mice. Disruption of BMP4 expression in the adipose tissue of Fabp4-cre-$BMP4^{loxP/loxP}$ mice was confirmed by Western blotting (Fig. S3*B*). The BMP4 mRNA level was not changed in brain, as determined by quantitative RT-PCR (qRT-PCR) (Fig. S3*C*).

Knockout mice gained more body weight (Fig. S3*D*) and exhibited increased WAT mass and fat index (fat weight relative to body weight) (Fig. 6 *A* and *B*), as well as adipocyte enlargement (Fig. 6 *C* and *D*). Unexpectedly, BAT of the BMP4-knockout mice also was hypertrophic and was associated with markedly increased fat mass and fat droplets in brown adipocytes (Fig. 6 *A*–*D*). Although the expression of mitochondrial and fatty acid oxidation-related genes (UCP-1, PGC1α, mtTFA, Cycs, CPT1b, and MCAD) did not decrease significantly, the expression of the white adipocyte genes for transcription factor 21 (Tcf21) (16) and leptin did increase in inguinal WAT (Fig. S3*E*). phosphorylated p38 and phosphorylated AFT2 (p-ATF2) were not activated in inguinal WAT of BMP4 knockouts as shown by Western blot (Fig. S3*F*). Metabolic parameter analysis revealed that BMP4-knockout mice also exhibited increased serum triglyceride levels but unchanged free fatty acid and cholesterol levels (Fig. 6 *E*–*G*). Serum leptin levels of BMP4-knockout mice also were markedly elevated (Fig. 6*H*). Fasting glucose and insulin levels were significantly elevated in knockout mice relative to controls (Fig. 6 *I* and *J*). Glucose tolerance tests revealed that knockout mice exhibited decreased glucose clearance (Fig. 6*K*). Although not statistically significant, the insulin tolerance curve for knockout mice was up-shifted (Fig. 6*L*). Consistent with the effects of BMP4 in TG mice, these findings indicate decreased insulin responsiveness in BMP4-knockout mice.

Discussion

Recent studies have shown that adult humans possess a pool of metabolically active brown fat that is susceptible to changes in environmental temperature (7–9). It follows that the identification of factors that induce BAT-like changes in WAT could lead to therapeutic strategies for treating obesity and its consequences. The present investigation reveals a connection between BMP4 and the transition of WAT to a tissue possessing white fat cells that have characteristics of brown fat cells, comparable to the recently described beige (14) and brite (15, 16) adipocyte cell types.

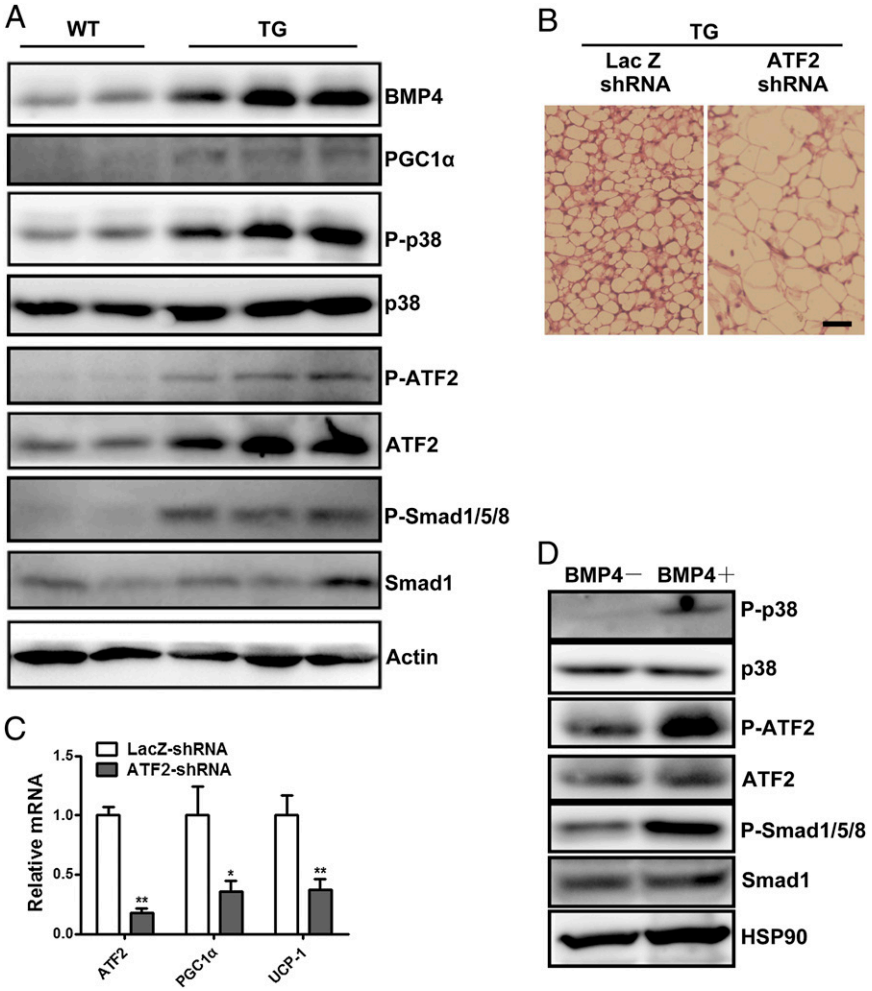

Fig. 5. Active metabolic WAT in Fabp4-BMP4 TG mice was regulated by the p38/MAPK/ATF2 pathway. (*A*) Western blot analysis of the expression level of molecules involved in the BMP-signaling pathway in inguinal WAT from 2-mo-old WT and Fabp4-BMP4 TG mice maintained on a chow diet. (*B*) H&E staining of inguinal WAT in the TG mouse after treatment with ATF2 or Lac Z shRNA. (Scale bar: 20 μm.) (*C*) qRT-PCR showing the fold induction of the expression of the indicated genes normalized to the housekeeping gene 18S in the inguinal WAT of the TG mouse after treatment with ATF2 or Lac Z shRNA (n = 4). The method of ATF2 shRNA adenovirus treatment was the same as the treatment with PGC1α shRNA in Fig. 4. (*D*) Western blot analysis of lysates (30 μg) from differentiated 3T3-L1 adipocytes at day 4 after MDI induction with or without BMP4 (20 ng/mL).

BMP4 is known to induce the commitment of pluripotent stem cells to the adipocyte lineage (32). Here we identify an additional role for BMP4 as a factor that produces BAT-like changes in WAT. Because the level of BMP4 in human WAT is inversely associated with fat mass (Fig. 1 *A* and *B*), its expression in WAT may serve as a therapeutic target. As shown in the present study, overexpression of BMP4 in adipose tissue in vivo in the mouse increases not only the number of SVF cells but also the number of adipocytes in both subcutaneous WAT and BAT. These results indicate that BMP4 stimulates proliferation as well as stem cell commitment to the adipocyte lineage (Fig. S1 *G* and *H*), most likely by an autocrine/paracrine mechanism, as was shown during commitment of multipotent C3H10T1/2 stem cells to preadipocytes in cell culture (32, 41).

It is noteworthy that we found that BMP4 also regulates adipose tissue remodeling, mitochondrial biogenesis, and metabolism. Driven by the adipocyte-specific Fabp4 promoter, overexpression of BMP4 in TG mice during terminal differentiation provoked acquisition of BAT characteristics in WAT (Figs. 1 *D* and *F* and 2). Furthermore, BMP4 treatment during terminal differentiation of 3T3-L1 preadipocytes induced similar changes (Fig. 2 *G*–*I*). These findings differ from previous reports in which humans and rodents were subjected to cold environment or noradrenergic stimulation and in which foci of UCP1-immunoreactive brown adipocytes appear in WAT. With noradrenergic stimulation, the foci were thought to involve direct transformation of adult white adipocytes (42–44) or de novo differentiation of committed brown adipocytes (45). It should also be noted that manipulation of certain genes that increased mitochondrial biogenesis in white adipocytes resulted in improved energy metabolism (18–20, 46). Likewise, overexpression of BMP4 in WAT promoted mitochondrial biogenesis as well as the expression of genes required for glucose and lipid metabolism, including Glut4, Pck-1, MCAD, and CPT1b (Fig. 2). These changes were associated with increased oxygen consumption, decreased blood levels of free fatty acid and triglycerides, and increased insulin responsiveness (Fig. 3). This phenotype also was verified in BMP4-knockout mice (Fig. 6). In contrast, in BMP4 TG mice lipid droplets in brown adipocytes were larger than in control mice (Fig. 1*F*), mitochondrial size decreased (Fig. 2*C*), and expression of genes of mitochondrial biogenesis and the enzymes for oxidative phosphorylation declined (Fig. 2*F*). These findings are consistent with the previous research showing that BMP4 inhibited UCP-1 expression of brown preadipocytes, differing from the role

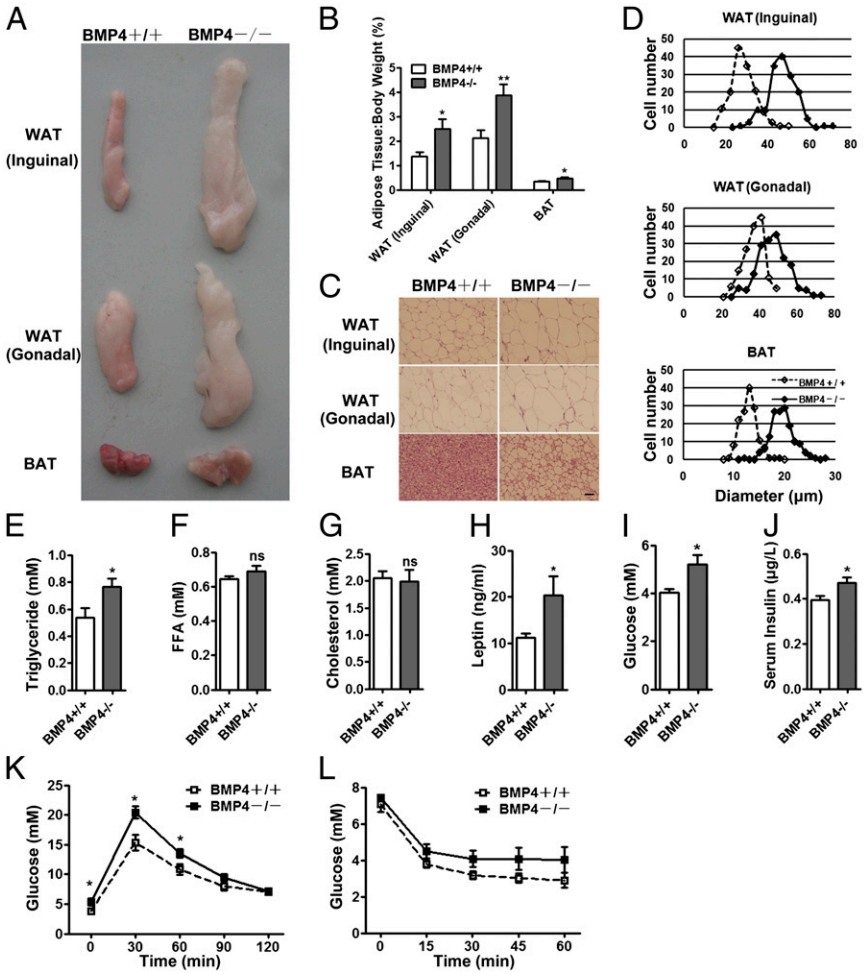

Fig. 6. BMP4-knockout mice had increased adipose tissue mass and reduced insulin sensitivity. (*A*) Comparison of inguinal WAT, gonadal WAT, and BAT in BMP4$^{+/+}$ (*Left*) and BMP4$^{-/-}$ (*Right*) mice. (*B*) Fat index (percentage of fat pad weight relative to the whole body weight) of inguinal WAT, gonadal WAT, and BAT in BMP4$^{+/+}$ and BMP4$^{-/-}$ mice (n = 7–8). (*C*) H&E staining of inguinal WAT, gonadal WAT, and BAT from BMP4$^{+/+}$ and BMP4$^{-/-}$ mice. (Scale bar: 20 μm.) (*D*) Quantification of cell size of inguinal WAT, gonadal WAT, and BAT in H&E-stained sections from three individual mice, five fields per mouse, 10–15 cells per field, using Image J software. (*E–H*) Fasting serum triglycerides (n = 6) (*E*), free fatty acid (FFA) (n = 7) (*F*), cholesterol (n = 8) (*G*), and leptin in BMP4$^{+/+}$ (n = 7) and BMP4$^{-/-}$ (n = 5) (*H*) mice. (*I* and *J*) Fasting serum glucose concentrations (n = 8) (*I*) and insulin concentrations (*J*) in BMP4$^{+/+}$ (n = 6) and BMP4$^{-/-}$ (n = 8) mice. (*K* and *L*) Glucose concentrations during an i.p. glucose tolerance test (n = 5) (*K*) or an insulin tolerance test (n = 5) (*L*) in BMP4$^{+/+}$ and BMP4$^{-/-}$ mice. BMP4$^{+/+}$, Fabp4-cre-BMP4$^{+/+}$; BMP4$^{-/-}$, Fabp4-cre-BMP4$^{loxP/loxP}$. Data from 6-mo-old mice on a normal chow diet are expressed as means ± SEM. $*P < 0.05$, $**P < 0.01$, $***P < 0.001$.

of BMP7 in brown adipocytes (30). The larger fat droplets in TG brown adipocyte BMP4 may have resulted from the diminished lipid dissipation.

Although expression of the typical BAT molecular marker UCP-1 was increased in the subcutaneous WAT of BMP4 TG mice, the level was somewhat lower than in typical interscapular brown adipose tissue (Fig. S2*A*). Moreover, some beige/brite markers (Tbx1, Tbx15, and Hoxc9) were increased in the tissue (Fig. 1*H*), suggesting that brown-like adipocytes transformed by BMP4 differ from typical brown adipocytes of interscapular BAT. This cell type may be related or identical to the beige and brite adipocyte cell types recently described by the Spiegelman (14) and Cannon (15, 16) laboratories, respectively. Nevertheless, the expression of PGC-1α in WAT (Fig. S2*B*), as well as p38/MAPK/ATF2 activation, was markedly elevated via BMP4 action (Fig. 5*A*), indicating that PGC-1α is a direct molecular effect of BMP4. Elevation of UCP-1 was secondary to PGC-1α stimulation.

Verification that PGC-1α is the key molecule was confirmed by the finding that inhibiting PGC1α expression (with PGC1a shRNA) caused multilocular small-sized adipocytes to revert to typical white adipocyte morphology (Fig. 4 *A–D*). The overexpression of BMP4 in mice robustly activated p38/MAPK and thus increased the level of both total ATF2 and p-ATF2 in WAT (Fig. 5*A*). In contrast, ATF2 knockdown caused the transformed brown-like adipocytes of BMP4 TG mice to revert to the normal white adipocyte phenotype (Fig. 5*B*). Together with the reported result of the transactivation of PGC-1α by ATF2 (47), these findings reveal the essential roles of p38/MAPK, ATF2, and PGC1α in the induction by BMP4 of an oxidative metabolic phenotype in WAT. Although BMP4 overexpression in BAT also activated the p38/MAPK/ATF2 pathway, the level of UCP-1 was lower than in control BAT. That BMP4 treatment decreased of UCP1 expression in cells differentiated from brown preadipocytes also was demonstrated by Tseng et al. (30). The decrease might be caused by the different key transcription factors or cofactors in WAT and BAT. In WAT development, BMP4 commits multipotent stem cells to preadipocytes primarily through activation of the Smad pathway, whereas induction to the brown-like adipocyte phenotype occurs primarily by activating the p38/MAPK pathway. Thus, complementary activation of the two signaling pathways appears to confer flexibility in BMP4's regulation

of adipose tissue development to meet metabolic demands at different points in development and metabolism (Fig. S3*G*).

It should be noted that in creating TG mice little control is exerted over the resulting level of expression of the transgene, which in most cases is high. The BMP4 transgene was expressed at a relatively high level (Fig. 1*C*), so the effects of the transgene may be exaggerated. However, this limitation is obviated, at least in part, by assessing the effect of disrupting the BMP4 gene. Of note, the BMP4 knockout was incomplete. As shown in Fig. S3*B*, a small, but significant, level of BMP4 was expressed in the BMP4-knockout mice. Also, as shown in Fig. S3*E*, the levels of expression of UCP-1, PGC1a, Cycs, CPT1b, and MCAD were all partially reduced in the BMP4-knockout mice, although the reductions did not achieve statistical significance. It is important that this group of genes was coordinately reduced. Had the knockout been total/complete, the relative levels of these reductions would have been expected to be greater.

Subcutaneous WAT and visceral WAT exert different levels of metabolic risks. Increased intraabdominal/visceral fat appears to exert a higher risk than subcutaneous fat. Hence, subcutaneous fat in the thighs and hips exhibits little risk of metabolic disease and even may have a protective effect (48, 49). Although PGC1α expression and mitochondrial biogenesis are increased in both tissue sites, inguinal WAT and gonadal WAT exhibit different phenotype upon BMP4 overexpression. Overexpression of BMP4 in gonadal WAT led to reduced adipocyte size and a reduction in the size of fat pads in mice between 2 and 6 mo of age (Fig. 1 *D–F* and Fig. S2*E*). In contrast, inguinal WAT mass did not change significantly between 2-mo-old and 6-mo-old in BMP4 TG mice (Fig. 1 *D* and *E* and Fig. S2*E*). Each of the molecules that uniquely affect BMP4 needs to be investigated further, especially those related to BMP4 and the insulin-signaling pathway. This alteration in fat mass suggests BMP4's protective role in metabolic disease and offers an opportunity for intervention in the control of excessive obesity.

Materials and Methods

Human Adipose Tissue Samples. Subcutaneous (n = 32) and visceral (omental) (n = 22) adipose tissues were obtained from patients who underwent surgery irrelevant to metabolic disease in Shanghai Jiaotong University Affiliated Sixth and Ninth People's Hospital. This study was approved by the ethics committees of Fudan University Shanghai Medical College and was in accordance with the principle of the Helsinki Declaration II. Written informed consent was obtained from each participant.

Generation of TG Mice Overexpressing Adipose Tissue-Specific BMP4 and BMP4-Knockout Mice. To generate mice with BMP4 specifically overexpressed in adipocytes, BMP4 cDNA (GenBank accession NM_007554) was cloned downstream of the 5.4-kb Fabp4 promoter/enhancer promoter and upstream of an SV40 intron/poly(A) sequence (50). The construct was microinjected into fertilized mouse (C57BL/6J x CBA/J F1) oocytes. BMP4 TG mice were screened by PCR using primers that specifically detect the transgene but not endogenous BMP4 (Fabp4-BMP4 Tg: cagtgatcattgccagggagaacc; gcctcctagcaggacttggcta). The TG founders were maintained by mating hemizygous animals to C57BL/6J mice. Control mice were non-TG littermates. To generate mice with an adipocyte-specific knockout of BMP4, Bmp4LoxP/LoxP mice (generously provided by Brigid Hogan, Department of Cell Biology, Duke University Medical Center, Durham, NC) were crossed with mice expressing Cre recombinase under the control of the adipocyte-specific promoter Fabp4 (Jackson Laboratory) (50). Genotyping was performed by PCR. Studies were performed in Fabp4-Cre-Bmp4LoxP/LoxP mice and littermate controls lacking the LoxP sites (Fabp4-Cre-Bmp4$^{+/+}$). Mice were maintained under 12-h light/12-h dark cycles with unlimited access to food and water. Mice were fed with chow or an HFD (51% kcal in fat, beginning at age 6 wk). The data shown were collected from experiments on male mice unless otherwise indicated. Fabp4-Bmp4 TG and non-TG WT mice from a C57BL/6J background were maintained by continuously crossing back, and Fabp4-Cre-Bmp4LoxP/loxP and Fabp4-Cre-Bmp4$^{+/+}$ mice were from a mixed background of C57BL/6J and 129/Black Swiss. Thus, slight variations between non-transgenic WT and Fabp4-Cre-Bmp4$^{+/+}$ values may reflect strain-specific differences. All studies were approved by the Animal Care and Use Committee of the Fudan University Shanghai Medical College and followed the National Institute of Health guidelines on the care and use of animals.

Glucose and Insulin Tolerance Tests. For the glucose tolerance test, mice were injected i.p. with D-glucose (2 mg/g body weight) after an overnight fast, and tail blood glucose levels were monitored. For the insulin tolerance test, mice fed ad libitum were injected i.p. with human insulin (Eli Lilly) (0.75 mU/g body weight) around 2:00 PM, and tail blood glucose levels were monitored.

Metabolic Studies. Three-month-old mice were housed and monitored individually in a metabolic cage (Columbia Instruments) with free access to regular chow and drinking water for 48 h. Each cage was monitored for metabolic parameters (including oxygen consumption and carbon dioxide production) at 25-min intervals throughout the 48 h period. Parameters of oxygen consumption (mL·kg^{-1}·h^{-1}), carbon dioxide production (mL·kg^{-1}·h^{-1}), and RER (CO_2/VO2) were calculated for each mouse divided by its body weight. Representative graphs of oxygen consumption and RER represent data for eight mice from each group.

Measurements of Blood Parameters. Mice at different ages were fasted overnight, and blood samples were collected by retroorbital bleeding methods. Sera were prepared and used for measurements. Glucose, triglycerides, and cholesterol levels were determined using the Sysmex Chemix-180 automatic biochemical analysis device (Sysmex Infosystems). ELISA kits were used to determine leptin (Raybiotech), insulin (Mercodia), and free fatty acid (Lengton Bioscience) levels in mouse sera.

H&E Staining and Cell Size Quantitation. Standard H&E staining was performed on 5-μm paraffin sections of WAT and interscapular brown adipose tissue. Cell diameter was measured in the H&E-stained sections of three individual samples in each group using Image J.

Isolation of SVF and Adipocytes from Adipose Tissue. Adipose tissue was harvested and the SVF cells were isolated by enzymatic digestion (collagenase VIII; Sigma). The digested tissue was filtered through a 100-μm mesh filter to remove debris and was centrifuged. The adipocytes floated above the supernatant. The cellular pellet involving the SVF was resuspended with an ammonium chloride lysis buffer to remove red blood cells.

Oil Red O and Nile Red Staining for Lipid. In vitro differentiated cells were fixed for 20 min in buffered formalin and stained with Oil Red O for 60 min. Isolated cells were resuspended in PBS, Nile red (stock: 0.5 mg/mL in acetone) was added to the preparation to effect a l:100 dilution, and cells were incubated for 5 min for flow cytometry.

Cell Culture and Induction of Adipogenesis. 3T3-L1 preadipocytes were plated at low density and cultured in DMEM containing 10% (vol/vol) calf serum. Two days postconfluence (designated day 0), cells were induced to differentiate with DMEM containing 10% (vol/vol) FBS, 1 μg/mL insulin, 1 μM dexamethasone, and 0.5 mM 3-isobutyl-1-methyl-xanthine until day 2. Cells then were fed with DMEM supplemented with 10% (vol/vol) FBS and 1 μg/mL insulin for 2 d, after which they were fed every other day with DMEM containing 10% (vol/vol) FBS. For BMP4 treatment, 20 ng/mL of purified recombinant BMP4 (R&D Systems) was added to the medium during the differentiation from day 0 to day 8.

qRT-PCR. cDNA synthesized from total RNA was analyzed in a Sequence Detector (Q5; Bio-Rad) with specific primers and SYBR Green PCR Master reagents (ABI). The relative abundance of mRNAs was calculated with 18S mRNA as the invariant control. The primers were from PrimerBank (http://pga.mgh.harvard.edu/primerbank/) or as described in refs. 14–16, 20, and 51.

Antibodies and Immunoblotting. WAT and BAT or cultured cells were homogenized in lysis buffer containing 2% (wt/vol) SDS and 60 mM Tris·HCl (pH 6.8) and were loaded onto the gel for electrophoresis. Proteins then were transferred onto nitrocellulose membrane and immunoblotted with specific antibodies. For determination of insulin-stimulated p-AKT, inguinal WAT was dissected from mice 5 min after i.p. injection of insulin. Antibodies used were BMP4 (Millipore), p38/MAPK, phos-p38/MAPK, Smad1, p-Smad1/5/8, Akt, and p-hr473-Akt (Cell Signaling Technology), actin (Sigma-Aldrich), PGC1α and HSP90 (Santa Cruz Biotechnology), and PRDM16 and UCP-1 (Abcam).

Adenoviral Expression Vectors and Infection. The adenoviral expression vector pBlock-it (Invitrogen) encoding shRNA of the PGC1α and ATF2 genes was constructed according to the manufacturer's protocols. The shRNA sequences were PGC1α: GGTGGATTGAAGTGGTGTAGA and ATF2: GTGAGGAGCCTT CTGTTGTA. Adenovirus was amplified and purified using Sartorius Adenovirus Purification Kits. Adenovirus solution was injected s.c. adjacent to the inguinal fat pad weekly for 4 wk in mice beginning at age 4 wk.

Statistical Analyses. All results are presented as means ± SEM. A nonpaired Student *t* test was used for these analyses. A difference was considered significant at $*P < 0.05$, $**P < 0.01$, and $***P < 0.001$.

ACKNOWLEDGMENTS. Fabp4-BMP4 TG mice were generated at Model Animal Research Center of Nanjing University. $BMP4^{LoxP/LoxP}$ mice were generously provided by Dr. Brigid Hogan. This research was supported in part by National Key Basic Research Project Grants 2011CB910201 and 2013CB530601, State Key Program of the National Natural Science Foundation Grant 31030048C120114, and Shanghai Key Science and Technology Research Project Grant 10JC1401000 (to Q.-Q.T.), and by National Natural Science Foundation Grant 30870510 (to X.L.). The Department of Biochemistry and Molecular Biology of Fudan University Shanghai Medical College is supported by Shanghai Leading Academic Discipline Project B110 and 985 Project 985III-YFX0302.

1. Scherer PE (2006) Adipose tissue: From lipid storage compartment to endocrine organ. *Diabetes* 55(6):1537–1545.
2. Klaus S (1997) Functional differentiation of white and brown adipocytes. *Bioessays* 19(3):215–223.
3. Shepherd PR, et al. (1993) Adipose cell hyperplasia and enhanced glucose disposal in transgenic mice overexpressing GLUT4 selectively in adipose tissue. *J Biol Chem* 268 (30):22243–22246.
4. Haslam DW, James WP (2005) obesity. *Lancet* 366(9492):1197–1209.
5. Kopelman PG (2000) Obesity as a medical problem. *Nature* 404(6778):635–643.
6. Kopecky J, Clarke G, Enerbäck S, Spiegelman B, Kozak LP (1995) Expression of the mitochondrial uncoupling protein gene from the aP2 gene promoter prevents genetic obesity. *J Clin Invest* 96(6):2914–2923.
7. van Marken Lichtenbelt WD, et al. (2009) Cold-activated brown adipose tissue in healthy men. *N Engl J Med* 360(15):1500–1508.
8. Virtanen KA, et al. (2009) Functional brown adipose tissue in healthy adults. *N Engl J Med* 360(15):1518–1525.
9. Cypess AM, et al. (2009) Identification and importance of brown adipose tissue in adult humans. *N Engl J Med* 360(15):1509–1517.
10. Frontini A, Cinti S (2010) Distribution and development of brown adipocytes in the murine and human adipose organ. *Cell Metab* 11(4):253–256.
11. English JT, Patel SK, Flanagan MJ (1973) Association of pheochromocytomas with brown fat tumors. *Radiology* 107(2):279–281.
12. Wilson-Fritch L, et al. (2004) Mitochondrial remodeling in adipose tissue associated with obesity and treatment with rosiglitazone. *J Clin Invest* 114(9):1281–1289.
13. Digby JE, et al. (1998) Thiazolidinedione exposure increases the expression of uncoupling protein 1 in cultured human preadipocytes. *Diabetes* 47(1):138–141.
14. Wu J, et al. (2012) Beige adipocytes are a distinct type of thermogenic fat cell in mouse and human. *Cell* 150(2):366–376.
15. Gburcik V, Cawthorn WP, Nedergaard J, Timmons JA, Cannon B (2012) An essential role for Tbx15 in the differentiation of brown and "brite" but not white adipocytes. *Am J Physiol Endocrinol Metab* 303(8):E1053–E1060.
16. Waldén TB, Hansen IR, Timmons JA, Cannon B, Nedergaard J (2012) Recruited vs. nonrecruited molecular signatures of brown, "brite," and white adipose tissues. *Am J Physiol Endocrinol Metab* 302(1):E19–E31.
17. Saito M, et al. (2009) High incidence of metabolically active brown adipose tissue in healthy adult humans: Effects of cold exposure and adiposity. *Diabetes* 58(7): 1526–1531.
18. Ahmadian M, et al. (2011) Desnutrin/ATGL is regulated by AMPK and is required for a brown adipose phenotype. *Cell Metab* 13(6):739–748.
19. Rousso-Noori L, et al. (2011) Protein tyrosine phosphatase epsilon affects body weight by downregulating leptin signaling in a phosphorylation-dependent manner. *Cell Metab* 13(5):562–572.
20. Nishino N, et al. (2008) FSP27 contributes to efficient energy storage in murine white adipocytes by promoting the formation of unilocular lipid droplets. *J Clin Invest* 118(8):2808–2821.
21. Morino K, et al. (2005) Reduced mitochondrial density and increased IRS-1 serine phosphorylation in muscle of insulin-resistant offspring of type 2 diabetic parents. *J Clin Invest* 115(12):3587–3593.
22. Ritov VB, et al. (2005) Deficiency of subsarcolemmal mitochondria in obesity and type 2 diabetes. *Diabetes* 54(1):8–14.
23. Vial G, Dubouchaud H, Leverve XM (2010) Liver mitochondria and insulin resistance. *Acta Biochim Pol* 57(4):389–392.
24. Puigserver P, et al. (1998) A cold-inducible coactivator of nuclear receptors linked to adaptive thermogenesis. *Cell* 92(6):829–839.
25. Yoon JC, et al. (2001) Control of hepatic gluconeogenesis through the transcriptional coactivator PGC-1. *Nature* 413(6852):131–138.
26. Wu Z, et al. (1999) Mechanisms controlling mitochondrial biogenesis and respiration through the thermogenic coactivator PGC-1. *Cell* 98(1):115–124.
27. Huss JM, Kopp RP, Kelly DP (2002) Peroxisome proliferator-activated receptor coactivator-1alpha (PGC-1alpha) coactivates the cardiac-enriched nuclear receptors estrogen-related receptor-alpha and -gamma. Identification of novel leucine-rich interaction motif within PGC-1alpha. *J Biol Chem* 277(43):40265–40274.
28. Vega RB, Huss JM, Kelly DP (2000) The coactivator PGC-1 cooperates with peroxisome proliferator-activated receptor alpha in transcriptional control of nuclear genes encoding mitochondrial fatty acid oxidation enzymes. *Mol Cell Biol* 20(5):1868–1876.
29. Patti ME, et al. (2003) Coordinated reduction of genes of oxidative metabolism in humans with insulin resistance and diabetes: Potential role of PGC1 and NRF1. *Proc Natl Acad Sci USA* 100(14):8466–8471.
30. Tseng YH, et al. (2008) New role of bone morphogenetic protein 7 in brown adipogenesis and energy expenditure. *Nature* 454(7207):1000–1004.
31. Whittle AJ, et al. (2012) BMP8B increases brown adipose tissue thermogenesis through both central and peripheral actions. *Cell* 149(4):871–885.
32. Tang QQ, Otto TC, Lane MD (2004) Commitment of C3H10T1/2 pluripotent stem cells to the adipocyte lineage. *Proc Natl Acad Sci USA* 101(26):9607–9611.
33. Martens K, Bottelbergs A, Baes M (2010) Ectopic recombination in the central and peripheral nervous system by aP2/FABP4-Cre mice: Implications for metabolism research. *FEBS Lett* 584(5):1054–1058.
34. Kajimura S, et al. (2009) Initiation of myoblast to brown fat switch by a PRDM16-C/EBP-beta transcriptional complex. *Nature* 460(7259):1154–1158.
35. Hondares E, et al. (2011) Peroxisome proliferator-activated receptor α (PPARα) induces PPARγ coactivator 1α (PGC-1α) gene expression and contributes to thermogenic activation of brown fat: Involvement of PRDM16. *J Biol Chem* 286(50):43112–43122.
36. Mootha VK, et al. (2003) PGC-1alpha-responsive genes involved in oxidative phosphorylation are coordinately downregulated in human diabetes. *Nat Genet* 34(3):267–273.
37. Seale P, et al. (2007) Transcriptional control of brown fat determination by PRDM16. *Cell Metab* 6(1):38–54.
38. Raz I, Eldor R, Cernea S, Shafrir E (2005) Diabetes: Insulin resistance and derangements in lipid metabolism. Cure through intervention in fat transport and storage. *Diabetes Metab Res Rev* 21(1):3–14.
39. Farmer SR (2008) Molecular determinants of brown adipocyte formation and function. *Genes Dev* 22(10):1269–1275.
40. Derynck R, Zhang YE (2003) Smad-dependent and Smad-independent pathways in TGF-beta family signalling. *Nature* 425(6958):577–584.
41. Bowers RR, Kim JW, Otto TC, Lane MD (2006) Stable stem cell commitment to the adipocyte lineage by inhibition of DNA methylation: Role of the BMP-4 gene. *Proc Natl Acad Sci USA* 103(35):13022–13027.
42. Granneman JG, Li P, Zhu Z, Lu Y (2005) Metabolic and cellular plasticity in white adipose tissue I: Effects of beta3-adrenergic receptor activation. *Am J Physiol Endocrinol Metab* 289(4):E608–E616.
43. Himms-Hagen J, et al. (2000) Multilocular fat cells in WAT of CL-316243-treated rats derive directly from white adipocytes. *Am J Physiol Cell Physiol* 279(3):C670–C681.
44. Barbatelli G, et al. (2010) The emergence of cold-induced brown adipocytes in mouse white fat depots is determined predominantly by white to brown adipocyte transdifferentiation. *Am J Physiol Endocrinol Metab* 298(6):E1244–E1253.
45. Schulz TJ, et al. (2011) Identification of inducible brown adipocyte progenitors residing in skeletal muscle and white fat. *Proc Natl Acad Sci USA* 108(1):143–148.
46. Zhang Y, et al. (2009) Adipose-specific deletion of autophagy-related gene 7 (atg7) in mice reveals a role in adipogenesis. *Proc Natl Acad Sci USA* 106(47):19860–19865.
47. Cao W, et al. (2004) p38 mitogen-activated protein kinase is the central regulator of cyclic AMP-dependent transcription of the brown fat uncoupling protein 1 gene. *Mol Cell Biol* 24(7):3057–3067.
48. Kissebah AH, Krakower GR (1994) Regional adiposity and morbidity. *Physiol Rev* 74(4): 761–811.
49. Wajchenberg BL (2000) Subcutaneous and visceral adipose tissue: Their relation to the metabolic syndrome. *Endocr Rev* 21(6):697–738.
50. Ross SR, et al. (1990) A fat-specific enhancer is the primary determinant of gene expression for adipocyte P2 in vivo. *Proc Natl Acad Sci USA* 87(24):9590–9594.
51. Hagberg CE, et al. (2010) Vascular endothelial growth factor B controls endothelial fatty acid uptake. *Nature* 464(7290):917–921.